2001 Proceedings of the 23rd Annual EMBS International Conference, October 25-28, Istanbul, Turkey

# NON-CONTACT MEASUREMENT OF THE ELECTRICAL IMPEDANCE OF BIOLOGICAL TISSUE

C.H. Riedel and O.Dössel

Institute of Biomedical Engineering, Universität Karlsruhe, Germany

**Abstract— The measurement of the impedance of biological tissue is a non-invasive method to find new data of diagnostic relevance. A change in the impedance for example can give a prediction of the healing process of wounds or of skin irritations [1]. The traditional way is to apply the current and measure the voltage with electrodes. This leads to stray capacitance between the electrodes as well as between the ground and patient at frequencies above 500 kHz. In the present report two sensitive systems are presented using computer simulations which can detect conductivity gradients. The systems are built up with two coils. In the first simulation the excitation coil is designed as a gradient coil to excite a magnetic field and a rectangular coil to measure. In the second simulation a rectangular coil is used as an exciting coil and a gradiometer coil is used to measure. The tissue block is divided into two halves with different conductivities. The sensors give no signal with a homogeneous tissue block. In precence of a conductivity gradient, the systems are sensitive. The main difference of the two systems is the geometrical arrangement of the eddy currents.**

*Keywords*—**contact-free measurement, electrical impedance, coil systems**

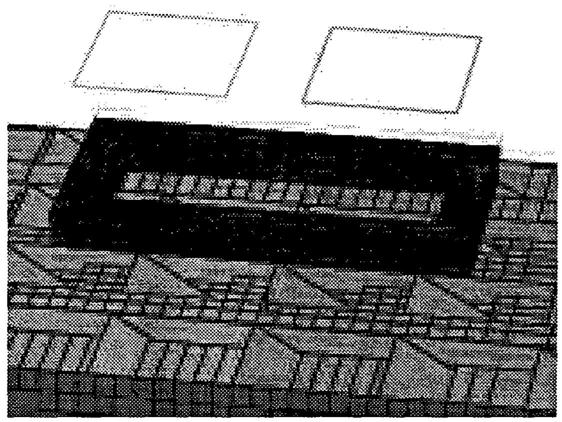

Fig. 1. Arrangement of the coil system and the tissue block. The excitation coil is simulated as two coils, the measurement coil is parallel underneath. The tissue is divided into two halves.

## I. Introduction

The non-invasive method of measuring the impedance can give information of the electrical characteristics of tissue. In some cases the conductivity gradient can be an important value. The diagnostic instrument could be a sensor, that is moved around on the skin of a patient, in order to detect areas with impedances that deviate from normal. If the patient has acute pain it is not possible to touch him, so a non-contact method must be used. In some applications (e.g. brain) impedance can hardly be measured with surface electrodes [2].

The non-contact measurement is based on the idea, that a time varying magnetic field induces eddy currents in the conductive tissue. These weaken the fields, so a change in the signal can be detected. Unfortunately the change in the signal is expected to be very small, so a high resolution is necessary [3]. In the present report two sensitive systems are presented and compared which are detecting a conductivity gradient.

## II. Methodology

An alternating current produces an alternating magnetic field. This magnetic field can be calculated using Biot-Savart's law. If this field passes through a conducting material eddy currents are induced. These eddy currents will also produce an alternating magnetic field, which weakens the original field, due to Lenz's law.

Different geometrical arrangements can be analyzed. [4] describes an analytical problem of a cylindrical coil with a three layer medium. [5] reduces the problem using a number of single coils. [6] gives a formula for the change of the signal in the measuring coil.

In this report a two coil system is used. The first is used as an excitation coil and the second is used as a measuring coil. For complex geometries a numerical method of field calculation, for example the finite integration method, can be used. Using simulations and calculations of different geometrical arrangements and different conductivities an ideal arrangement can be found.

The induced voltage $u_{\text{ind}}$ now depends on the distances, the geometrical arrangement and the conductivities of the tissue block. The calculation is done with the finite integral method. Two geometrical arrangements were simulated, both use a two coil system. The simulation is done with MAFIA [7]. Both the excitation and the measurement coil are in parallel and in parallel to the tissue underneath.

Fig. 1 shows the geometrical arrangement for the first simulation. In this case the excitation coil is designed as a gradiometer coil. Therefore two rectangular coils are used. The excitation current runs clockwise on the right and counter-clockwise on the left. The measuring coil is simulated as a rectangular coil, which is parallel to and underneath of the exci-

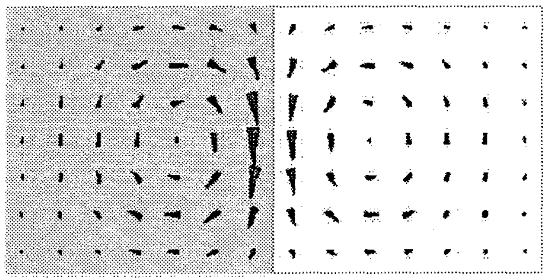

Fig. 2. Eddy currents in the tissue. A conductivity of 0.1 $\frac{1}{\Omega m}$ at the left and of 0.08 $\frac{1}{\Omega m}$ at the right are used and a gradiometer coil as an excitation coil is used.

tation coil. The implementation of the coil is made of discrete voxels. The cross section of the coil is 2 x 2 voxel. The tissue underneath is divided into two halves with different conductivities. The advantage of this geometric arrangement is, that the total flux which passes through the measuring coil is almost zero if there is no tissue or homogeneous tissue underneath. If there is different conductivity under the left and the right side, there will be eddy currents of different strengths.

Fig. 2 shows the eddy currents in the tissue block from above. In this simulation a conductivity of 0.1 $\frac{1}{\Omega m}$ on the left and 0.08 $\frac{1}{\Omega m}$ on the right is used. Therefore it is clear, that the eddy currents are higher in the area with low resistance. Because of Lenz's law these eddy currents will effect the excitation field. Because the tissue is divided, an asymmetrical shielding will take place.

Fig. 3 shows the second geometrical arrangement used. Here the excitation coil is simulated as a rectangular coil. The measuring coil is simulated in the shape of an eight, which lies in between the excitation coil and the tissue block. Because the eight

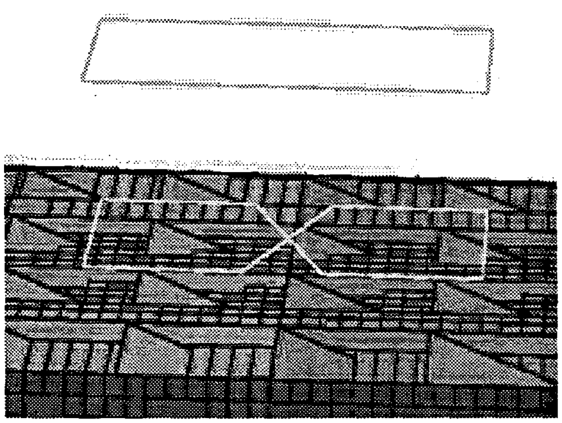

Fig. 3. Arrangement of the coil system and the tissue block. The excitation coil is simulated as a rectangular coil, the measurement coil is parallel underneath in the shape of an eight. The tissue is divided into two halves.

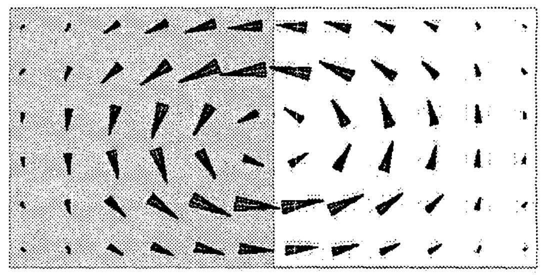

Fig. 4. Eddy currents in the tissue. A conductivity of 0.1 $\frac{1}{\Omega m}$ at the left and of 0.08 $\frac{1}{\Omega m}$ at the right are used and a rectangular coil as an excitation coil is used.

needs to lay plain, the measuring coil was simulated as filaments instead of discrete voxels.

Fig. 4 shows the eddy currents in the tissue block from above. Also in this simulation a conductivity of 0.1 $\frac{1}{\Omega m}$ on the left and 0.08 $\frac{1}{\Omega m}$ on the right is used. As before it is clear that the eddy currents have a different shape in the area with low resistance as compared to the other side.

In practice the induced voltage is measured. The measured current $I_{\text{meas}}$ and the measured voltage $U_{\text{meas}}$ can be calculated from the fields.

$$U_{\text{meas}} = \int \vec{E}^* \vec{ds} \tag{1}$$

$$I_{\text{meas}} = \oint \vec{H}^* \vec{ds} \tag{2}$$

Here $\vec{E}^*$ is the electric field and $\vec{H}^*$ the magnetic field. Both are solved in frequency domain and therefore are complex values.

## III. Results

The following results were achieved with a simulation using an excitation current of 1 A and a frequency of 500 kHz. In this simulation the distance of the measuring and the excitation coil was varied. Because constant eddy currents are desired, the distance of the exciting coil and the tissue was held

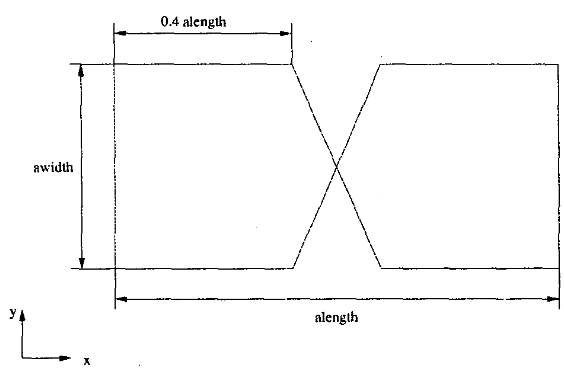


Fig. 5. Geometrical arrangement of the measuring coil in the shape of an eight.

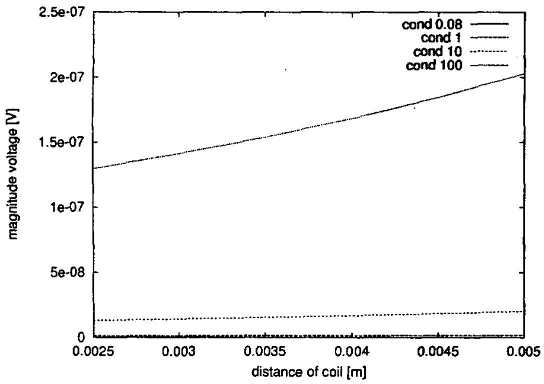


Fig. 6. Magnitude of the voltage in dependence on the distance from the measuring coil to the excitation coil. The conductivity was varied from 0.08 $\frac{1}{\Omega \mathrm{m}}$ to 100 $\frac{1}{\Omega \mathrm{m}}$ on the left and a conductivity of 0.1 $\frac{1}{\Omega \mathrm{m}}$ on the right was used. A gradiometer coil is used as an excitation coil.

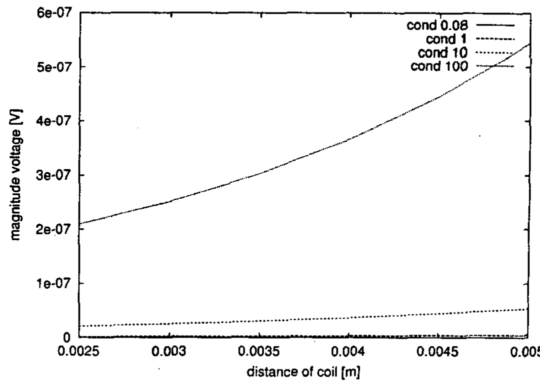


Fig. 8. Magnitude of the voltage in dependence on the distance from the measuring coil to the excitation coil. The conductivity was varied from 0.08 $\frac{1}{\Omega \mathrm{m}}$ to 100 $\frac{1}{\Omega \mathrm{m}}$ on the left side and a conductivity of 0.1 $\frac{1}{\Omega \mathrm{m}}$ on the right was used. A rectangular coil is used as an excitation coil.

constant at 6 mm. For the rectangular a geometry of coil 10 x 5 mm is used. The gradiometer coil was simulated with two coils and each coil has a size of 4 x 5 mm. When the gradiometer coil is in the shape of an eight the geometric values of Fig. 5 are used. Here *alength* is 10 mm and *awidth* 5 mm. The mesh has a higher resolution in the area of the coils.

Fig. 6 and Fig. 7 show the magnitude of the voltage when a gradiometer coil is used as an excitation coil. Fig. 6 shows tissues with high conductivity to demonstrate the principle and Fig. 7 uses physiological values. In this simulation the distance of the measuring and the excitation coil was varied. The conductivity on the left side was varied from 0.08 $\frac{1}{\Omega \mathrm{m}}$ to 100 $\frac{1}{\Omega \mathrm{m}}$. The right conductivity was held constant at 0.1 $\frac{1}{\Omega \mathrm{m}}$. So a conductivity step was realized in the contact area. Fig. 6 shows that there is a difference in the signal, and the difference is greater if the measuring coil is located nearer to the tissue. This makes sense, because the coupling is higher, if it is nearer. Tests with a geometry without a tissue block or with a homogeneous tissue result in a voltage $U_{\mathrm{meas}}$ of $1\mathrm{e}^{-14}$ V.

Fig. 8 and Fig. 9 show the magnitude of the induced voltage when a rectangular coil is used as an excitation coil. Fig. 8 shows cases with a high conductivity step to demonstrate the principle and Fig. 9 uses physiological values. The same conductivity values as before are used. The simulation without a tissue block or with homogeneous tissue results in a signal of the same order of magnitude as before.

If the two geometrical arrangements are compared, Fig. 6 and Fig. 8 present the same sensitivity but the ascending slope in Fig. 8 is higher and the distance plays a greater role.

The second important aspect is the geometrical

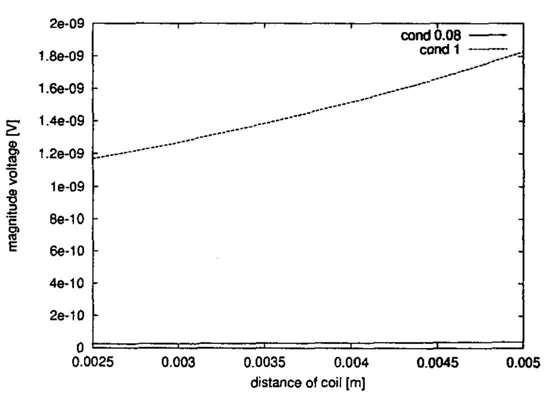


Fig. 7. Magnitude of the voltage in dependence on the distance from the measuring coil to the excitation coil. The conductivity was set at 0.08 $\frac{1}{\Omega \mathrm{m}}$ and 1 $\frac{1}{\Omega \mathrm{m}}$ on the left and a conductivity of 0.1 $\frac{1}{\Omega \mathrm{m}}$ on the right was used. A gradiometer coil is used as an excitation coil.

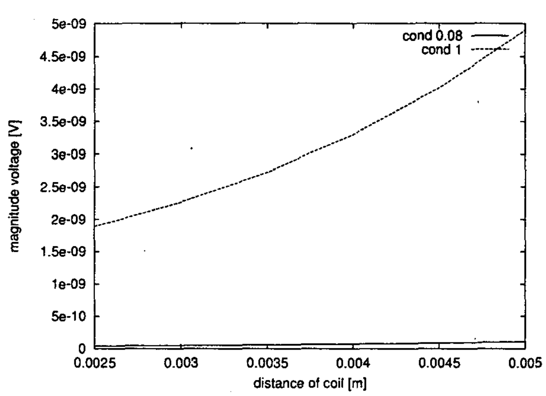


Fig. 9. Magnitude of the voltage in dependence on the distance from the measuring coil to the excitation coil. The conductivity was set at 0.08 $\frac{1}{\Omega \mathrm{m}}$ and 1 $\frac{1}{\Omega \mathrm{m}}$ on the left and a conductivity of 0.1 $\frac{1}{\Omega \mathrm{m}}$ on the right was used. A rectangular coil is used as an excitation coil.

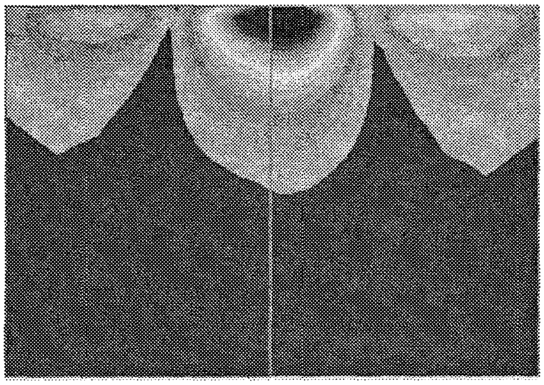

Fig. 10. Eddy currents in the tissue. A conductivity of 0.1 $\frac{1}{\Omega m}$ at the left and of 0.08 $\frac{1}{\Omega m}$ at the right are used and a gradiometer coil as an excitation coil is used.

arrangement of the eddy currents. In Fig. 2 a greater density and a compact arrangement is obtained. Fig. 10 shows the magnitude of the current in the tissue. The tissue block is cut in the middle and the two sides with different conductivities can be seen. A conductivity of 0.1 $\frac{1}{\Omega m}$ at the left and of 0.08 $\frac{1}{\Omega m}$ at the right are used and a rectangular coil as an excitation coil is used. The scale of the currents value ranges from 0 to 5e-3 A.

Fig. 4 shows an extensive spread of eddy currents. Fig. 11 shows as before the magnitude of the currents in the tissue. The same conductivities were used as before, only a rectangular coil as an excitation coil is used.

Fig. 11 and Fig. 10 also show the difference in deepness of the eddy currents in the tissue. If the conductivity gradient is higher the shape changes extremely and the currents mostly flow in one side.

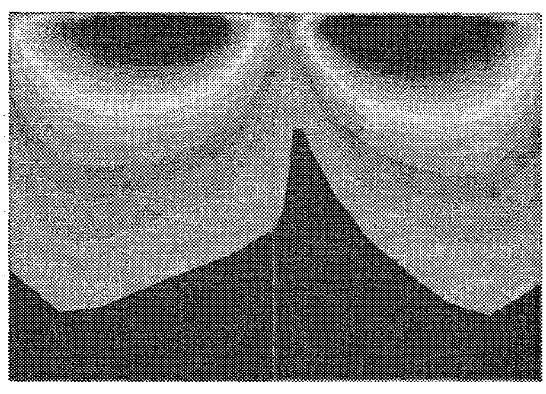

Fig. 11. Eddy currents in the tissue. A conductivity of 0.1 $\frac{1}{\Omega m}$ at the left and of 0.08 $\frac{1}{\Omega m}$ at the right are used and a rectangular coil as an excitation coil is used.

## IV. Discussion

The non-contact measurement of biological impedances is based on the measurement of small changes in the magnetic field $\vec{H}$. These changes creat a small signal in the detector coil. Therefore a high resolution must be used. To find an absolute value of the conductivity the exact geometry must be known. If the gradient of conductivity is to be determined the measuring sensor can be more sensitive, because the signal start from zero.

## V. Conclusion

The numerical simulation confirmed the expected result. A step of 0.02 $\frac{1}{\Omega m}$ in the tissue below the sensor results in a measurable signal. The signal is higher, if the sensor is nearer to the tissue. If the two arrangements are compared, the simulation shows that both result in a signal of the same order of magnitude. The main difference is the geometrical arrangement of the eddy currents. So a special sensor can be designed for a specific region of interest.


## Acknowledgment

The author wish to thank Marc-André Golombeck at the Universität Karlsruhe (TH) for discussion and help in MAFIA that were of great value to this work. The work was sponsored by Ministerium für Wissenschaft, Forschung und Kunst Baden-Württemberg.


## References


[1] I. Nicander, B. L. Rozell, L. Rundquist, and S. Ollmar, "Electrical impedance. a method to evaluate subtle changes of the human oral mucosa," *European J Oral Sciences*, vol. 105, pp. 576–582, 1997.

[2] H. Hutten, H. Scharfetter, W. Ninaus, B. Puswald, G. I. Petrova, and D. Kovachev, "Inductively coupled wideband transceiver for bioimpedance spectroscopy (IBIS)," in *Proceedings of the 20th Annual Conference of the IEEE Engineering in Medicine and Biology Society*, vol. 20, pp. 1791–1794, 1998.

[3] H. Scharfetter, H. K. Lackner, and J. Rosell, "High resolution hardware for magnetic induction tomography (MIT) at low frequencies," in *Proceedings of the EIT Conference in London (in Press)*, 2000.

[4] P. Wach, "Theoretische Untersuchung der Rückwirkung der Wirbelströme," *Zeitschr. für Elektrotechnik und Maschinenbau ; Zeitschr. d. Österreichischen Verbandes für Elektrotechnik*, vol. 76, pp. 505–509, 1979.

[5] A. V. Korzenevskii and V. A. Cherpenin, "Magnetic induction tomography," *J Communications Technology and Electronics*, vol. 42, no. 4, pp. 469–474, 1997.

[6] H. Griffiths, W. R. Stewart, and W. Gough, "Magnetic induction tomography," in *Electrical Bioimpedance Methods: Applications to Medicine and Biotechnology* (P. J. Riu, J. Rosell, R. Bragós, and Ó. Casas, eds.), vol. 873, pp. 335–345, New York: The New York Academy of Sciences, 1999.

[7] T. Weiland and M. Bartsch, "Mafia version 4.," in *Proc. of the Computational Accelerator Physics Conference (CAP)*, pp. 65–70, 1996.